

Controlling Stimulated Brillouin Backscatter with Beam Smoothing in Weakly Damped Systems

Laurent Divol

L-399, Lawrence Livermore National Laboratory, University of California, P. O. Box 808, California 94551, USA
(Received 5 June 2007; published 9 October 2007)

We derive an analytical estimate of the effect of temporal smoothing of laser beams on stimulated Brillouin scattering (SBS) in a regime relevant to indirect drive ignition. We predict a strong reduction of SBS in the gold plasma expanding from the *Hohlraum* wall with temporal smoothing. This is a new regime far above threshold where the time to reach convective saturation allows for an effective contrast reduction of the beam intensity driving the instability. This result agrees with three dimensional simulations. Polarization smoothing is shown to double the effective bandwidth.

DOI: [10.1103/PhysRevLett.99.155003](https://doi.org/10.1103/PhysRevLett.99.155003)

PACS numbers: 52.38.Bv, 02.50.Ey, 52.35.Mw

Much work has been devoted to studying the mitigation of backscattering instabilities with laser beam smoothing schemes. For the temporal problem, the three time scales of the problem are the laser bandwidth $\Delta\omega$, the linear growth of the instability γ_0 and the damping rate of the acoustic wave [for stimulated Brillouin scattering (SBS)] involved, ν . Early work [1] used perturbation theory in regimes where $\Delta\omega \gg \gamma_0$. It was then shown that the so-called Bourret approximation applies, and the typical result was to replace ν by $\nu + \Delta\omega$, leading to an increase of the SBS threshold. These early results looked mainly at phase modulation and typical bandwidths required were in the tens of nanometers, out of reach for fusion applications. On the other hand, spatial smoothing using random phase plates [2] became common on large laser facilities in the early 1990s, as it allowed control over the laser focal spot shape and increased shot reproducibility. Most studies focused on the effect of localized overintensities, or speckles, generated by spatial smoothing on backscattering instabilities. Experimental results [3] and models [4] showed that one could expect large reflectivities (indeed a divergent result in the linear steady-state framework) for an average linear gain exponent as low as 1 over a speckle length (hence the definition of a critical intensity). The technological limit on bandwidth for 1- μm light being around 1 nm for fusion applications, no direct effect of temporal smoothing on backscattering instabilities was expected as $\Delta\omega < \gamma_0$ and mitigation of filamentation or other slower laser-plasma coupling processes was invoked to explain experimental results [5]. Beyond perturbation theory, it was suggested [6,7] that temporal smoothing could still affect backscattering instabilities if the laser correlation time $\tau_c \equiv \Delta\omega^{-1}$ is shorter than the convective saturation time for the instability. This was observed in numerical simulations [8] and confirmed by theory [9] near the critical threshold for SBS in the strongly damped regime.

In this Letter, we derive an analytical model that describe the effects of temporal smoothing on SBS in a short plasma (less than a speckle long) when the average SBS linear gain is much larger than 1 and the average linear

growth rate is larger than the laser bandwidth ($\gamma_0\tau_c > 1$). These conditions correspond to a region of high risk for SBS in indirect drive ignition targets: the *Hohlraum* Au-wall blowoff. The laser power deposited in the wall for x-ray conversion creates a hot plasma expansion over a few hundred microns. Competition between absorption, rising density and decreasing temperatures limits the SBS prone region to one or two speckle lengths. Experimental results obtained at NOVA and numerical simulations [10] have suggested that temporal smoothing can have a direct mitigation effect on SBS in this regime. Typical parameters are $T_e \approx T_i = 3\text{--}5$ keV, $n_e/n_c = 0.1\text{--}0.2$ for a gold plasma ($Z \approx 60$). Laser intensity is $I_0 \approx 0.5\text{--}5 \times 10^{14}$ W \cdot cm $^{-2}$ in the Au plasma and a speckle length is $L_{\text{sp}} = 8f^2\lambda_0 = 140$ μm for the projected target designs at the National Ignition Facility (NIF) [11], assuming an $f/8$, $\lambda_0 = 0.351$ μm laser beam. With these parameters, $\gamma_0 \approx 0.5\text{--}1.5$ ps $^{-1}$ and $\nu = 0.06$ ps $^{-1}$, the linear SBS gain for amplitude $g_0 = \gamma_0^2 L_{\text{sp}}/\nu c \approx 5\text{--}15$ is well above the critical gain where SBS reflectivity could occur. Typical bandwidths available on the next generation of laser facilities are around $\Delta\omega = 270$ Ghz (at 3ω) giving a correlation time $\tau_c \approx 3$ ps. In this regime where $\gamma_0\tau_c \approx 4 \gg 1$ and $g_0 \gg 1$, no model exists to quantify the effect of temporal smoothing on SBS.

We consider the following one-dimensional (1D) description of SBS

$$c\partial_x a_1 - \gamma_0 a_2 = 0; \quad (\partial_t + \nu)a_2 - \gamma_0 a_1 = S, \quad (1)$$

$$\gamma_0^2 = \frac{1}{16} \frac{v_{\text{osc}}^2}{v_e^2} \frac{n_e}{n_c} \frac{\omega_a \omega_0}{1 + k_a^2 \lambda_{\text{De}}^2}, \quad (2)$$

a_1 is the backscattered (light) wave and a_2 is the SBS-driven (acoustic) wave. We have assumed infinite speed of light, which limits us to correlation times $\tau_c > L_{\text{sp}}/c \approx 0.5$ ps. In this regime, the backscattered light instantaneously reacts to the SBS-driven acoustic wave variations. We have neglected the advection of acoustic waves at the sound speed c_s , which will affect the long time behavior of SBS in the absolutely unstable regime. With the above parameters, the absolute threshold is $2\gamma_0/\nu > \sqrt{c/c_s}$ or

$I_0 > 2.5 \times 10^{14} \text{ W} \cdot \text{cm}^{-2}$. We then expect our results to be valid for all intensities at times shorter than the convective saturation time $g_0/\nu \approx 150 \text{ ps}$, and for intensities below the absolute threshold at later times. We also note that weak gradients in plasma parameters are likely to hinder any absolute growth, while not affecting our results.

Let us pose $x \equiv x/L_{\text{sp}}$ and $t \equiv \nu t$. The Green functions of interest are solution of $\partial_x G^1 - g_0^{1/2} G^2 = 0$; $(\partial_t + 1)G^2 - g_0^{1/2} G^1 = \delta(x)\delta(t)$. These are $G^2(x, t) = H(t)e^{-t}\delta(x) + H(x)e^{-t}\sqrt{g_0 t/x}I_1(2\sqrt{g_0 x t})$ and $G^1(x, t) = H(x)e^{-t}\sqrt{g_0}I_0(2\sqrt{g_0 x t})$.

To model temporal smoothing, we assume that the laser intensity I_n changes every $\tau_c \approx \Delta\omega^{-1}$, follows exponential statistics $p(I_n) = \exp(-I_n/I_0)$ and that the intensities

I_n at different time steps are independent, which is correct over one full oscillation of the frequency modulator (f_{fm}^{-1}) for smoothing by spectral dispersion (SSD [12]) or always for ISI-like smoothing schemes [6]. Figure 1 shows the distribution of the laser intensity averaged over f_{fm}^{-1} at the best focus of an $f/8$ smoothed beam varying the SSD bandwidth. Our simple model gives a probability distribution for the time-averaged intensity

$$P(\langle I \rangle_{f_{\text{fm}}^{-1}} = x) = n_f e^{-n_f x} \frac{(n_f x)^{n_f - 1}}{(n_f - 1)!}, \quad (3)$$

where $n_f = (f_{\text{fm}}\tau_c)^{-1}$ is the depth of modulation. The best fit between the simulated field and our model is obtained with $\tau_c = 0.83\Delta\omega^{-1}$. The formal solution to (1) is then $a_2(n\tau_c) = \sum_{i=1}^n \Gamma_n^i$, where

$$\Gamma_n^i \equiv \prod_{k=n}^i G_k * S = \int_0^1 \dots \int_0^1 G_n(1 - x_n)G_{n-1}(x_n - x_{n-1}) \dots \int_0^{\tau_c} G_i(x_{i+1} - x_i, t) dt dx_i \dots dx_n \quad (4)$$

and $G_n(x) = G^2(x, t = \tau_c, I = I_n)$. Now looking at the dominant contribution R_n to the driven acoustic wave amplitude $a_2(n\tau_c)$, in the limit $g_0\tau_c > 1$, as the x_i are ordered in the previous multiple integral due to the Heaviside function in the Green function, we have

$$R_n \equiv \Gamma_n^1 \approx \int \dots \int \exp\left[\sum_{i=1}^n 2\sqrt{g_i\tau_c a_i} - n\tau_c\right] da_1 \dots da_n, \quad (5)$$

with $a_i > 0$ and $\sum a_i = 1$. A saddle point approximation around $a_i = g_i / \sum_{k=1}^n g_k$ finally gives

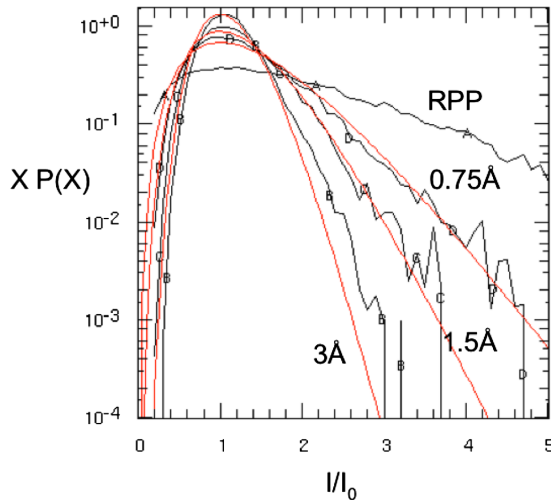


FIG. 1 (color online). Power distribution $IP(I)$ time averaged over a full SSD cycle for a 17 GHz modulator and various laser bandwidth. The red lines correspond to our model Eq. (3) and the black curves to the corresponding simulated laser field using a $128 \times 128\lambda_0$ simulation box. As little as 0.75 Å of bandwidth has a significant effect on the high-intensity tail of this distribution.

$$\langle R_n \rangle \simeq e^{-n\tau_c} \int_0^\infty e^{\alpha\sqrt{x}} P(X = x) dx, \quad (6)$$

where the average is done over realizations of the laser field. $\alpha = 2\sqrt{g_0\tau_c}$ and $X \equiv \sum_{k=1}^n I_k$. For $n < n_f$, $P(x) = e^{-x}x^{n-1}/(n-1)!$ and

$$\langle R_n \rangle = e^{-n\tau_c} \{M(n, 1/2, \alpha^2/4) + \alpha[\Gamma(n + 1/2)/\Gamma(n)]M(n + 1/2, 3/2, \alpha^2/4)\}. \quad (7)$$

Using an asymptotic expression for the confluent hypergeometric function M when n is large, $M(a, b, z) \approx_{a \rightarrow \infty} e^{z/2} J_{b-1}(\sqrt{2bz - 4az})$ leads to

$$\langle R_n \rangle \simeq e^{g_0\tau_c/2} e^{\sqrt{(4n-1)g_0\tau_c}} e^{-n\tau_c}. \quad (8)$$

This is the main result of this Letter. One can see that the average response of the stochastic system (1) at time $n\tau_c$ is the deterministic response obtained when using the average laser intensity times $\exp(g_0\tau_c/2)$. This later term then describes the effect of high-intensity speckles generated by the spatial smoothing of the beam. The maximum amplification is given by $\max_n[\langle R_n \rangle] \propto \exp g_0(1 + \tau_c/2)$ and is reached when $n = n_{\text{sat}} = g_0/\tau_c$, leading to the same convective saturation time as Eq. (1) using the average laser intensity. When $\tau_c \rightarrow \infty$, the average response diverges as expected from the spatial smoothing only result when pump depletion is neglected. When $\tau_c \rightarrow 0$, one recovers the response to the average laser intensity. For experimental observables, one is interested in the average backscattered intensity which is given by $R \propto \exp[2g_0(1 + \tau_c)]$. Figure 2 shows the expected effect of SSD on SBS using this result and a simple Tang [13] formula to account for pump depletion: $R(1 - R) = \epsilon \exp[2g_0(1 + \tau_c)(1 - R)]$, $\epsilon = 10^{-9}$. One can see a dramatic effect of SSD on SBS as soon as the laser bandwidth is similar to the damping of the acoustic waves ($\tau_c \approx 1$), even if $\Delta\omega < \gamma_0$. While the instantaneous growth rate of the instability is faster than the laser frequency modulation, time averaging of the laser

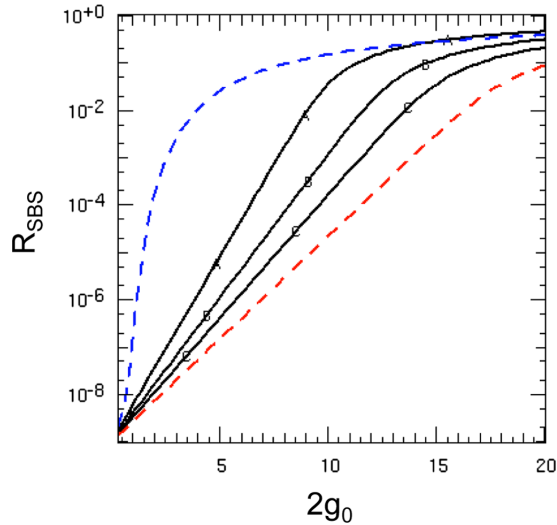


FIG. 2 (color online). Effect of temporal smoothing on SBS reflectivity as predicted by our model for $\tau_c = 0.8$ (A), 0.4 (B), and 0.2 (C) as a function of the linear gain. This corresponds to 0.75 , 1.5 , and 3 \AA of bandwidth at $1 \mu\text{m}$ wavelength. The dashed blue line is the steady-state result (spatial smoothing only [4]) while the red dashed line is the result for a plane wave (no speckles, lowest reflectivity).

intensity occurs over the many e folding necessary to reach convective saturation, thus decreasing the contrast of the intensity pattern and diminishing the role of high-intensity speckles.

Another beneficial effect of temporal smoothing is to reduce statistical fluctuations, which means improved shot reproducibility in experiments. It is well known that spatial smoothing leads to a very large standard deviation for the near-threshold reflectivity, putting doubts on the meaning of its average value [14]. This is due to the dominant contribution of very intense (and rare) speckles. With temporal smoothing, using Eq. (6) at convective saturation time, $n = n_{\text{sat}}$, the reflectivity is dominated by the time-averaged laser intensity pattern around $(1 + 2\tau_c)I_0$. Figure 1 shows that this is well sampled even by a small laser spot. Using Eq. (8), the standard deviation for the reflectivity is $\sigma = e^{2g_0\tau_c}$. For our typical parameters, $\sigma \approx 100$, but a typical laser spot is a few hundred microns wide and contains $N_{\text{sp}} \gg 10^4$ speckles, so that ensemble averaging gives an effective standard deviation $\sigma/N_{\text{sp}}^{1/2} < 1$ and justify the use of Eq. (8) as a predictor for the measured reflectivity.

An additional beam smoothing technique is polarization smoothing [15], which is implemented on NIF. This technique instantaneously reduces the contrast of the laser intensity pattern by 2. Using the same model with $P(I_n) = 4I_n \exp(-2I_n/I_0)$, one readily obtains $R_{\text{PS}} \propto \exp(2g_0(1 + \tau_c/2))$. While using PS alone still leads to a divergent result for the 1D linear model as soon as $g_0 > 1$ (i.e., significant reflectivity if pump depletion is included), it doubles the effective bandwidth when temporal smoothing is added, which can strongly reduce SBS for g_0 as large as 8–10.

All the previous results are valid when the saturation time of the convective growth is shorter than a frequency modulator cycle $g_0/\nu < f_{\text{fm}}^{-1}$. For our typical parameters this is true for a 10 GHz modulator, but not for the NIF 17 GHz modulator. To model the cyclic recurrence of the intensity pattern generated by SSD, we let $I_n = I_{n \equiv n_f}$. After n_c cycles (i.e., $n = n_c \times n_f$), $P(X_n) = P(X_{n_f}/n_c)/n_c$, which means that the contrast of the time-averaged intensity pattern does not decrease after one cycle. What matters then is whether the instability saturates before one cycle. One can write the effect of the laser bandwidth on the reflectivity as

$$R \propto \exp[2g_0(1 + g_0/N)]; \quad N = \min(n_{\text{sat}} \equiv g_0/\tau_c, n_f). \quad (9)$$

N is the number of successive uncorrelated intensity patterns generated by SSD at best focus during the growth of SBS. It is worth noting that while the effect of SSD on backscatter is directly related to the total bandwidth of the laser when $N < n_f$, the maximum effect is related to the depth of modulation n_f . One should note that self-smoothing effects or adding a second low frequency modulator (3 GHz on NIF) can break the cyclic recurrence of intense speckles and should lead to ISI-like smoothing schemes.

This model can now be compared to three dimensional simulations of SBS performed with the code PF3D [16]. This code solves the complete set of three dimensional coupled-wave equations describing SBS, including the diffraction and finite advection effect neglected in Eq. (1). It also includes a realistic description of spatial (random phase plates), temporal (SSD), and polarization smoothing. We used plasma and laser parameters consistent with those listed in the introduction. We chose $T_e = 3 \text{ keV}$, $Z = 60$, $T_i = 2 \text{ keV}$, and $n_e/n_c = 0.2$, assuming an $f/8$, $0.351 \mu\text{m}$ laser beam. This gives $\gamma_0(\text{ps}^{-1}) = 0.9\sqrt{I_{14}}$, $\nu(\text{ps}^{-1}) = 0.07$. The absolute threshold is $I_{14} \equiv I/10^{14} \text{ W} \cdot \text{cm}^{-2} > 2.7$ and we limit ourselves to intensities below this threshold. The 1D amplitude linear gain is $g_0 = 7I_{14}$. 1D-SSD was implemented using a 17 GHz modulator and up to 3 \AA of bandwidth at $1 \mu\text{m}$. It was critically dispersed. Figure 3(a) shows a typical instantaneous laser intensity pattern in the plasma. The brightest speckles are up to 10 times the average intensity. Figure 3(b) shows the same laser intensity pattern averaged over a modulation cycle when 3 \AA of SSD is applied, showing vertical streaks due to the one-dimensional nature of SSD. The contrast is reduced with peak intensity features at 3 times the average. Figures 3(c) and 3(d) shows the driven acoustic waves and resulting backscattered light at the same time as Fig. 3(a). As predicted by our model, these are strongly correlated with the time-averaged laser pattern and show little contribution from single bright speckles. Figure 4 summarizes the simulations' results. The time-averaged SBS reflectivity is plotted function of the laser average intensity for various SSD bandwidths.

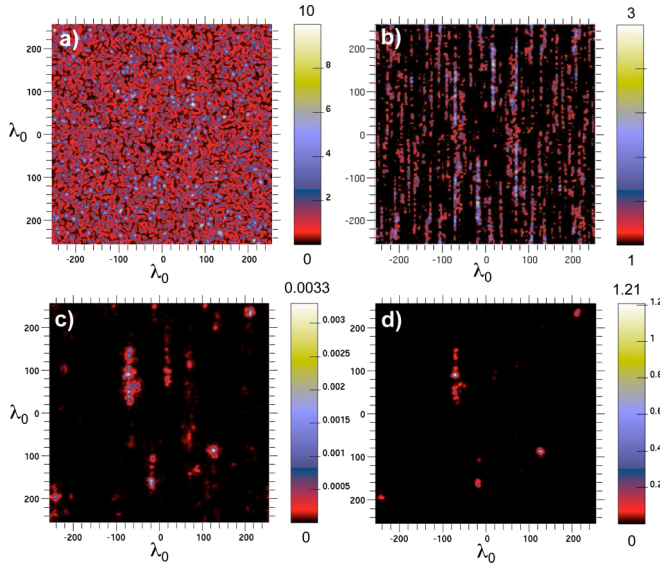


FIG. 3 (color online). (a) Instantaneous laser intensity pattern in the plasma as simulated by PF3D. The intensity is normalized to the average intensity. (b) Same laser intensity pattern averaged over a modulation cycle when 3 Å of SSD is applied. (c),(d) The SBS-driven acoustic waves ($\delta n_e/n_e$) and resulting backscattered light at the same time as (a). The bright vertical features coinciding on (b),(c) and (d) indicate that SBS is correlated with the time-averaged intensity pattern (b).

These simulations were run until a statistical steady state was reached (typically $2n_{\text{sat}}\tau_c \approx 200$ ps). The average reflectivity exhibits an exponential growth with intensity, the amplification rate decreasing with laser bandwidth. The error bars on simulation results come from fluctuations in time and sampling of the theoretical intensity distribution from different simulations. The solid lines are derived from Eq. (9) as $R = \epsilon \exp[2g_0(1 + g_0/n_f)]$ with $\epsilon = 10^{-10}$. Here, $n_f = 18$, $\tau_c = 0.2$, and $n_{\text{sat}} = 35$ for 3 Å of SSD at $I_{14} = 1$. A spatially smoothed beam can produce significant reflectivity for g_0 as low as 4 ($I = 0.6$) due to the contribution of very intense speckles, while adding 3 Å of SSD moves this threshold to $I = 1$. As little as 1.5 Å of SSD can strongly reduce SBS in the intermediate gain regime $g_0 \approx 5$. As predicted, adding polarization smoothing amount to doubling the depth of modulation. Also, as $n_{\text{sat}} > n_f$ for 1.5 Å of SSD at $I_{14} = 0.75$, using a 8.5 GHz modulator with twice the depth of modulation to obtain 1.5 Å of bandwidth leads to a significant reduction of the reflectivity.

In this Letter, we have derived an analytical model for the effect of temporal smoothing on SBS in a new regime relevant to upcoming attempts at indirect drive inertial fusion. In a short plasma with weak Landau damping, corresponding to the high Z material used for x-ray conversion, and where the linear gain is much larger than unity, we have shown that a small amount of laser band-

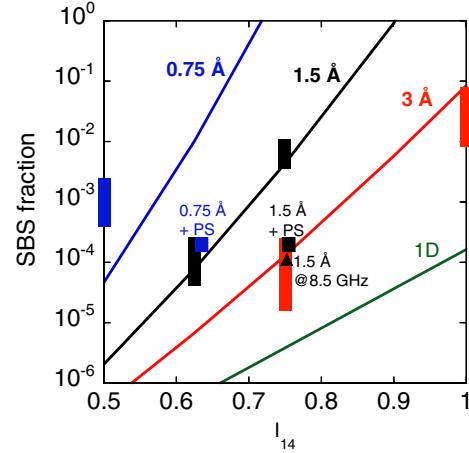


FIG. 4 (color online). Comparison of SBS reflectivity from PF3D simulations (bars) and our model (lines) for 0.75 (blue), 1.5 (black), and 3 Å (red) of SSD bandwidth. Bars' spread corresponds to statistical variations between different simulations. The squares represent simulations with PS, showing it doubles the effective bandwidth. The triangle is a PF3D simulation with an 8.5 GHz modulator and twice the depth of modulation. The green line corresponds to the plane wave case (zero contrast).

width can strongly reduce the reflectivity from a spatially smoothed laser beam. Our model agrees well with detailed three dimensional simulations and further predicts that using polarization smoothing doubles the effective laser bandwidth in this regime.

The author would like to thank B. Langdon, E. A. Williams, and R.L. Berger for useful discussions. This work was performed under the auspices of the U.S. Department of Energy by the Lawrence Livermore National Laboratory under Contract No. W-7405-ENG-48.

- [1] G. Laval *et al.*, Phys. Fluids **20**, 2049 (1977); E. A. Williams *et al.*, Phys. Fluids **22**, 139 (1979).
- [2] Y. Kato *et al.*, Phys. Rev. Lett. **53**, 1057 (1984).
- [3] S. P. Obenshain *et al.*, Phys. Rev. Lett. **62**, 768 (1989).
- [4] H. A. Rose *et al.*, Phys. Rev. Lett. **72**, 2883 (1994).
- [5] S. H. Glenzer *et al.*, Phys. Plasmas **7**, 2585 (2000).
- [6] A. N. Mostovych *et al.*, Phys. Rev. Lett. **59**, 1193 (1987).
- [7] P. M. Guzdar *et al.*, Phys. Fluids B **3**, 2882 (1991).
- [8] R. L. Berger *et al.*, Phys. Plasmas **6**, 1043 (1999).
- [9] Ph. Mounaix *et al.*, Phys. Rev. Lett. **85**, 4526 (2000).
- [10] S. H. Glenzer *et al.*, Phys. Rev. Lett. **80**, 2845 (1998); Nature Phys. (to be published).
- [11] J. D. Lindl *et al.*, Phys. Plasmas **11**, 339 (2004).
- [12] S. Skupsky *et al.*, J. Appl. Phys. **66**, 3456 (1989).
- [13] C. L. Tang, J. Appl. Phys. **37**, 2945 (1966).
- [14] Ph. Mounaix *et al.*, Phys. Rev. Lett. **89**, 165005 (2002).
- [15] S. Pau *et al.*, J. Opt. Soc. Am. B **11**, 1498 (1994).
- [16] R. L. Berger *et al.*, Phys. Plasmas **5**, 4337 (1998).